

Functional connectivity analysis of multiplex muscle network across frequencies

Author:

Kerkman, JN; Daffertshofer, A; Gollo, LL; Breakspear, M; Boonstra, TW

Publication details:

Proceedings of the Annual International Conference of the IEEE Engineering in Medicine and Biology Society, EMBS
v. 2017

Medium: Print

pp. 1567 - 1570

9781509028092 (ISBN)

1557-170X (ISSN); 1558-4615 (ISSN)

Event details:

39th Annual International Conference of the IEEE Engineering in Medicine and Biology Society (EMBC)

Seogwipo, South Korea

2017-07-11 - 2017-07-15

Publication Date:

2017-09-14

Publisher DOI:

<https://doi.org/10.1109/EMBC.2017.8037136>

License:

<https://creativecommons.org/licenses/by-nc-nd/4.0/>

Link to license to see what you are allowed to do with this resource.

Downloaded from http://hdl.handle.net/1959.4/unsworks_47514 in <https://unsworks.unsw.edu.au> on 2024-04-26

Functional connectivity analysis of multiplex muscle network across frequencies*

Jennifer N. Kerkman, Andreas Daffertshofer, Leonardo L. Gollo, Michael Breakspear, and Tjeerd W. Boonstra

Abstract— Physiological networks reveal information about the interaction between subsystems of the human body. Here we investigated the interaction between the central nervous system and the musculoskeletal system by mapping functional muscle networks. Muscle networks were extracted using coherence analysis of muscle activity assessed using surface electromyography (EMG). Surface EMG was acquired from 36 muscles distributed throughout the body while participants were standing upright and performing a bimanual pointing task. Non-negative matrix factorization revealed functional connectivity in four frequency bands. The spatial arrangement differed considerably across frequencies supporting a multiplex network organisation. Graph-theory analysis of layer-specific network revealed a consistent fat-tail distribution of the edges weights, distinct efficiency values, and core-periphery properties. These frequency bands may be spectral fingerprints of different neural pathways that innervate the spinal motor neurons to control the musculoskeletal system.

I. INTRODUCTION

The human organism is an integrated network, in which complex physiological systems, each with its own regulatory mechanisms, continuously interact. By mapping the interactions among diverse systems, one can identify physiological networks [1]. Network analysis has been applied to different physiological systems in the search for understanding how dynamical interactions may result in collective functional behaviour. This includes, for example, studies on interactions between heart rate variability and electroencephalography (EEG) rhythms to examine the control of autonomic cardiac activity during sleep [2]. Network analysis has proven crucial for examining how multiple spatially distinct brain regions interact to enable cognitive functioning and control behaviour [3].

More recently, network analysis has been shown useful to unravel interactions between the central nervous system and the musculoskeletal system. The musculoskeletal system can be cast as a network in which muscles are linked to one another by the bones they are connected to [4, 5]. The nerv-

ous system has to coordinate activity of multiple muscles when controlling the musculoskeletal system, as changes in muscle activity in one part of the body may also affect other muscle groups. This coordination can be investigated by mapping functional muscle networks based on intermuscular coherence [6]. Intermuscular coherence reflects synchronized neural inputs to different muscles, which can be used to infer the neural pathways that project to spinal motor neurons [7].

Here we investigated the organisation of functional muscle networks in human subjects who performed a postural task. We used non-negative matrix factorisation (NNMF) to distinguish oscillatory inputs at different frequencies and investigate the resulting network topology at each frequency band. Every frequency band forms a layer of a multiplex network [8]. As we will argue, these layers encode distinct types of interactions between muscles and thereby facilitate both parallel and hierarchical structures for motor control.

II. METHODS

Functional muscle networks were determined of seven male and seven female healthy subjects (25 ± 8 years). To induce activity in muscles across the whole body, subjects were instructed to stand upright while pointing on a target in front of them holding a laser pointer with two hands. The Ethics Committee Human Movement Sciences of the Vrije Universiteit Amsterdam had approved the study (reference ECB 2014-78).

Bipolar electromyography (EMG) was measured from 36 muscles distributed across the whole body, i.e. 18 bilateral muscles: tibialis anterior (TA), gastrocnemius medialis (GM), soleus (SOL), rectus femoris (RF), biceps femoris (BF), vastus lateralis (VL), adductor longus (AL), external oblique (EO), pectoralis major (PMA), sternocleidomastoideus (SMA), longissimus (LO) latissimus dorsi (LD), trapezius (TZ), deltoid (D), biceps brachii (BB), triceps brachii (TRB), extensor digitorum (ED), flexor digitorum superficialis (FDS). EMG envelopes were extracted via the Hilbert transform before determining the pairwise complex-valued coherency of all 630 muscle pairs. For every subject coherencies were averaged over trials.

The squared modulus of the coherency spectra (magnitude-squared coherences) were decomposed in four components using NNMF such that components show minimal overlap in their frequency range, which are peaked at the different frequency bands [6]. The advantage of using NNMF is that extracted spectral profiles and weights that define the muscle networks are semi-positive definite, that is, the adjacency matrices are semi-positive definite as re-

*Research supported by the Netherlands Organization for Scientific Research (NWO #45110-030 and #016.156.346).

J. N. Kerkman and A. Daffertshofer are with the Faculty of Behavioural and Movement Sciences, Vrije Universiteit Amsterdam, Amsterdam, the Netherlands (phone: +31 20 5988579; e-mail: j.n.kerkman@vu.nl, a.daffertshofer@vu.nl).

L. L. Gollo and M. Breakspear are with QIMR Berghofer Medical Research Institute, Brisbane, Australia (e-mail: leonardo.l.gollo@gmail.com, mjbreaks@gmail.com).

T. W. Boonstra is with the Black Dog Institute, University of New South Wales, Sydney, Australia (phone: +61 2 9382 9285; e-mail: t.boonstra@unsw.edu.au).

quired for the majority of commonly used network metrics [6, 9]. The corresponding NNMF-weights yielded undirected weighted graphs per frequency component. By construction, these four graphs connected the same set of nodes and hence formed the layers of a multiplex network, here referred to as a muscle network.

For every subject, the weighted muscle networks were thresholded to create binary networks. We used a relative threshold of 0.058 ± 0.013 (mean-value over subjects \pm SD) guaranteeing a minimally-connected network across frequencies without isolated nodes; all muscles were connected to at least one other muscle by an edge at one of the layers of the multiplex network in every subject. Since we used the same relative threshold across frequencies, the network density is identical across layers.

To quantify the multiplex networks, we computed the network metrics ‘mean degree’ [9] and ‘core/periphery structure’ (‘maximized coreness’) [10] for each network layer using the Brain Connectivity Toolbox [9]. We also estimated ‘global efficiency’ via Dijkstra’s algorithm [11]. Differences between layers were tested using an ANOVA with repeated measures.

III. RESULTS

NNMF yielded four modes in distinct frequency ranges spanning, from here-on denoted as 0-3, 3-11, 11-21, and 21-60 Hz frequency ‘layer’, respectively. The corresponding weights, which served to define the weighted connectivity matrix, appeared to follow a power law indicating a scale-free topology at each layer of the multiplex network (Fig. 1).

We found clear differences in the spatial arrangement of edges (Fig. 2, left column). These differences became particularly visible after thresholding the edges to create the aforementioned minimally-connected binary networks (Fig. 2, right column). For example, the 3-11 Hz layer contained several connections between distinct body segments, whereas the 21-60 Hz layer predominantly covered connections between muscles within the same body segment (Fig. 3).

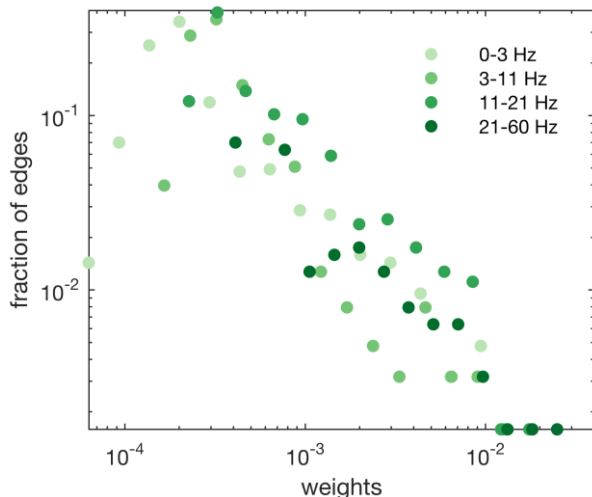


Figure 1. Distribution of weighted edges of the four frequency layers averaged over subjects.

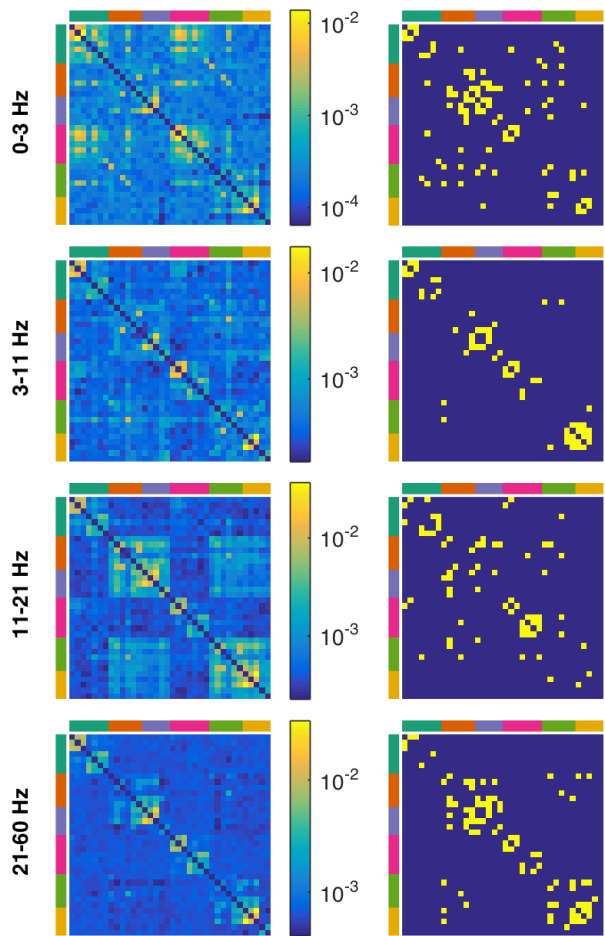


Figure 2. Adjacency matrices of the four layers of the muscle networks averaged over subjects: log transformed weighted networks (left column) and minimally-connected binary networks (right column). Colours on bars along axes indicate leg, trunk and arm muscles at the right and the left side, respectively.

The core-periphery structure revealed distinct core subdivision across layers. In the 0-3 Hz layer, the core consisted mainly of muscles in the legs and lower back. In the 3-11 Hz layer, this core subdivision changed from legs and lower back to a combination of legs and trunk, to trunk and arms in 11-21 Hz, and to a more segregated subdivision in the 21-60 Hz layer (Fig. 3). As a result, the maximized coreness changed significantly across these frequency components, $F(3,39)=13.90$, $p<.001$, $\eta_p^2=0.52$. The 0-3 Hz and 11-21 Hz layers revealed very high maximized coreness (0.93 ± 0.15 and 0.75 ± 0.17), as the core of the network was located in either the legs and lower back or in the arms, respectively. In the other two layers (3-11 and 21-60 Hz), the core was more spread across the body, accompanied by a lower maximized coreness (0.63 ± 0.19 and 0.60 ± 0.09).

The degree distribution also differed considerably across layers. Comparing the degree of each muscle (node) across frequencies, visual inspection revealed that several muscles mainly participated in a particular layer (frequency component) of the network (Fig. 4). For example, leg muscles, in particular GM and SOL in the lower leg and BF in the upper leg, had a high degree at the lowest frequencies (0-3 Hz). In

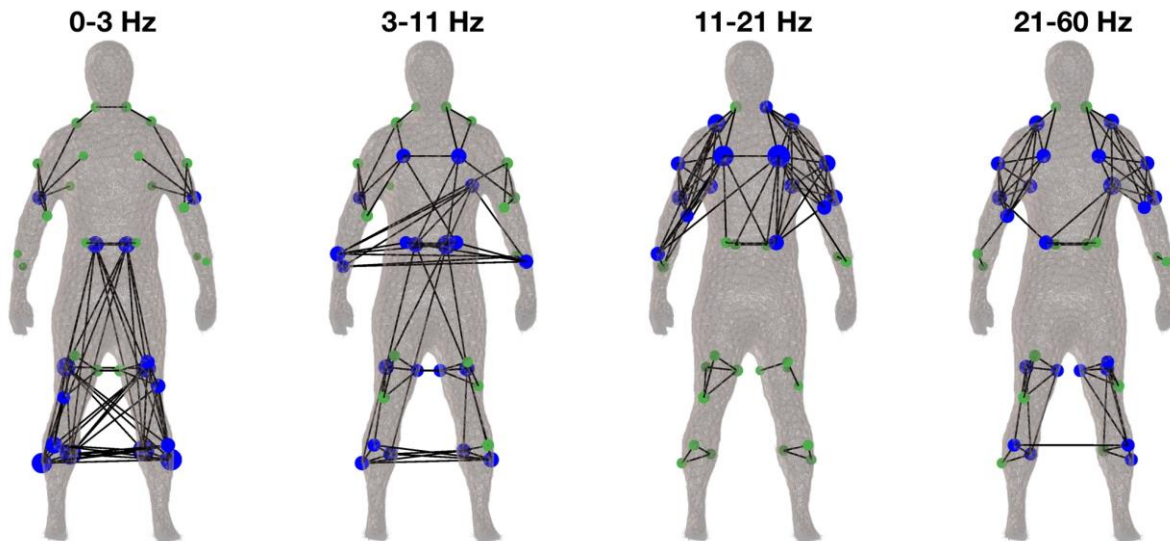


Figure 3. Spatial representation of the four layers of the multiplex network averaged over subjects. Edges represent the minimally-connected network (relative threshold of 0.052) across frequency components. Color-coding shows the core-periphery structure (blue: core nodes, green periphery nodes) and the size of the edges is relative to the degree of the node. Body meshes obtained from [18].

contrast, the forearm muscles ED and FDS were completely uncoupled from this layer and instead showed the highest degree at 3-11 Hz. Chest (PMA) and shoulder muscles (TZ, D) had the highest degree in the 11-21 Hz layer, while the degrees in the 21-60 Hz layer were more evenly distributed across muscles, in line with our findings regarding the core-periphery structure.

The global efficiency changed significantly from 0.12 ± 0.04 to 0.16 ± 0.08 , 0.12 ± 0.05 and 0.15 ± 0.09 from the layer of the lowest to that of the highest frequencies ($F(3,39)=3.79$, $p=0.02$, $\eta_p^2=0.23$).

IV. DISCUSSION

Functional connectivity analysis of EMG envelopes revealed connectivity in distinct frequency bands, which yielded the layers of the multiplex network. Networks dif-

fered significantly across layers as demonstrated by several network metrics. The lowest frequency layer (0-3 Hz) contained a network connecting primarily leg muscles, as reflected by their degree and core subdivision. The second layer (3-11 Hz) contained more uniform connectivity across muscles and displayed a lower coreness statistic. The forearm muscles participated particularly to this layer. The third layer (11-21 Hz) showed again a high maximized coreness statistic, which mainly involved trunk and arm muscles. The fourth layer (21-60 Hz) had the lowest coreness statistic and was dominated by a uniform and local connectivity. These findings demonstrate that functional muscle networks can form a multiplex network and that, if following this approach, the layers in the multiplex contain networks with different, anatomically plausible, spatial arrangements in distinct frequency ranges.

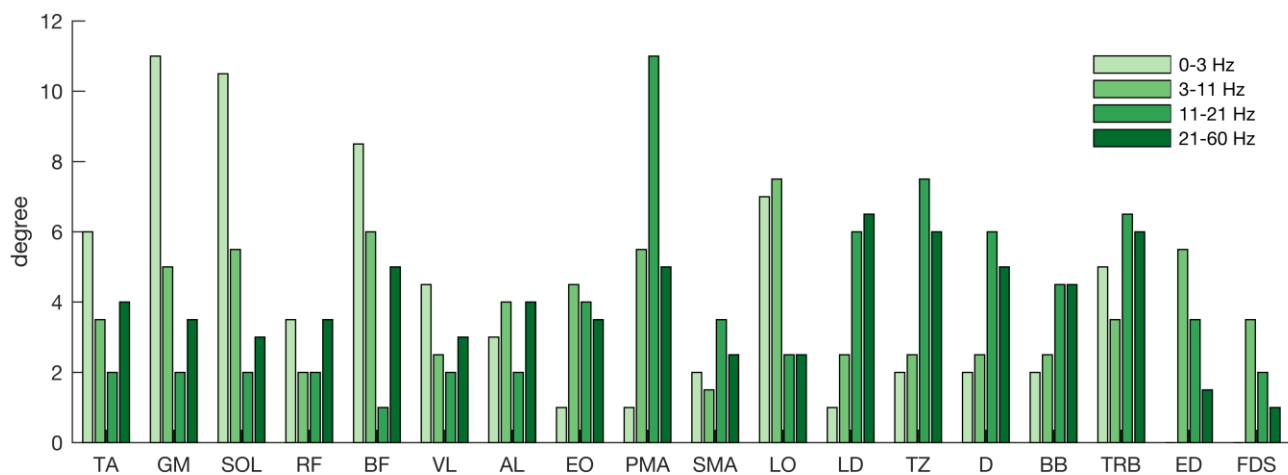


Figure 4. Degree distribution for the four frequency layers of the multiplex network, averaged over homologous muscles (on the left and right side of body) and subjects.

The layers of the functional muscle network likely reflect different types of interactions between the central nervous system and the musculoskeletal system. Previous studies reported functional connectivity between sensorimotor systems at particular frequencies. When it comes to interactions between motor cortex and muscles, corticomuscular coherence has been mainly observed in the beta frequency band (15-30 Hz) [12, 13], while intermuscular coherence between homologous muscles is dominant in the alpha band (6-12 Hz) [14]. This separation in frequencies suggests different mechanisms underlying the emergence of the coherence patterns. One possibility for this is the involvement of two separate neural pathways with direct corticospinal projections and divergent projections to the musculoskeletal system originating from subcortical regions such as the olivocerebellar system [15]. Here we advocate the analysis of multiplex muscle networks as it may provide information about the wiring diagrams of different neural pathways that project to the spinal motor neurons in parallel, which would be lost when analysing a single frequency or collapsing networks across different frequencies. By using model inversion techniques the functional connectivity patterns of each layer may be used to uncover structural pathways in the motor system that are otherwise difficult to assess directly [16].

When focussing on spinal cord activity, so-called motor synergy encoders may also help explaining the emergence of the different layers of muscle network, as they have proven successful in the analysis of muscle synergies [17]. They receive input from both the motor cortex and sensory pathways and target motor unit pools through a combination of direct monosynaptic connections and indirect polysynaptic connection through a motor synergy encoder network. The inter-segmental axons of motor synergy encoders allow for activating non-neighbouring and even distant motor neurons. Connectivity between muscles located close to and far away from each other can hence reflect the organisation of these synergy encoders in the spinal cord.

To experimentally probe for mechanisms underlying muscle networks, perturbing the networks and monitoring their changes appears as an obvious next step. How do multiplex network change in different behavioural conditions, for example, when the stability of the subject is jeopardized? In fact, changes in tasks conditions have already been shown to affect a single muscle network [6], but it remains to be seen whether this also alters the multiplex structure reported here. In any case, this future work will further underscore the value of multiplex networks in studying physiological networks.

V. CONCLUSION

Intermuscular coherence reveals functional connectivity at multiple broadband, but distinct frequency components that give rise to a multiplex network organisation. The corresponding network metrics display different characteristics between the layers of this multiplex network. This uncovers the anatomically plausible structures of correlated oscillatory inputs to muscles across frequencies and provides novel insight into the neural pathways that are involved in the coordination of the musculoskeletal system.

REFERENCES

- [1] A. Bashan, R. P. Bartsch, J. W. Kantelhardt, S. Havlin, and P. C. Ivanov, "Network physiology reveals relations between network topology and physiological function," *Nat. Commun.*, vol. 3, p. 702, 2012.
- [2] L. Faes, G. Nollo, F. Jurysta, and D. Marinazzo, "Information dynamics of brain-heart physiological networks during sleep," *New J. Phys.*, vol. 16, no. 10, p. 105005, 2014.
- [3] E. Bullmore and O. Sporns, "Complex brain networks: graph theoretical analysis of structural and functional systems," *Nat. Rev. Neurosci.*, vol. 10, no. 3, pp. 186–198, 2009.
- [4] B. Esteve-Altava, R. Diogo, C. Smith, J. C. Boughner, and D. Rasskin-Gutman, "Anatomical networks reveal the musculoskeletal modularity of the human head," *Sci. Rep.*, vol. 5, p. 8298, 2015.
- [5] A. C. Murphy, S. F. Muldoon, D. Baker, A. Lastowka, B. Bennett, M. Yang, and D. S. Bassett, "Structure, Function, and Control of the Musculoskeletal Network," *arXiv Prepr. arXiv 1612.06336*, 2016.
- [6] T. W. Boonstra, A. Danna-Dos-Santos, H. B. Xie, M. Roerdink, J. F. Stins, and M. Breakspear, "Muscle networks: Connectivity analysis of EMG activity during postural control," *Sci. Rep.*, vol. 5, p. 17830, 2015.
- [7] T. W. Boonstra and M. Breakspear, "Neural mechanisms of intermuscular coherence: implications for the rectification of surface electromyography," *J. Neurophysiol.*, vol. 107, no. 3, pp. 796–807, 2012.
- [8] M. De Domenico, S. Sasai, and A. Arenas, "Mapping multiplex hubs in human functional brain networks," *Front. Neurosci.*, vol. 10, 2016.
- [9] M. Rubinov and O. Sporns, "Complex network measures of brain connectivity: Uses and interpretations," *Neuroimage*, vol. 52, no. 3, pp. 1059–1069, 2010.
- [10] S. P. Borgatti and M. G. Everett, "Models of core/periphery structures," *Soc. Networks*, vol. 21, no. 4, pp. 375–395, 2000.
- [11] E. W. Dijkstra, "A note on two problems in connexion with graphs," *Numer. Math.*, vol. 1, no. 1, pp. 269–271, 1959.
- [12] B. A. Conway, D. M. Halliday, S. F. Farmer, U. Shahani, P. Maas, A. I. Weir, and J. R. Rosenberg, "Synchronization between motor cortex and spinal motoneuronal pool during the performance of a maintained motor task in man," *J. Physiol.*, vol. 489, no. 3, p. 917, 1995.
- [13] C. v. d. Steeg, A. Daffertshofer, D. F. Stegeman, and T. W. Boonstra, "High-density surface electromyography improves the identification of oscillatory synaptic inputs to motoneurons," *J. Appl. Physiol.*, vol. 116, no. 10, pp. 1263–1271, 2014.
- [14] T. W. Boonstra, B. C. M. van Wijk, P. Praamstra, and A. Daffertshofer, "Corticomuscular and bilateral EMG coherence reflect distinct aspects of neural synchronization," *Neurosci. Lett.*, vol. 463, no. 1, pp. 17–21, 2009.
- [15] I. E. J. de Vries, A. Daffertshofer, D. F. Stegeman, and T. W. Boonstra, "Functional connectivity in neuromuscular system underlying bimanual muscle synergies," *J. Neurophysiol.*, vol. 116, no. 6, pp. 2576–2585, 2016.
- [16] T. W. Boonstra, S. Farmer, and M. Breakspear, "Using computational neuroscience to define common input to spinal motor neurons," *Front. Hum. Neurosci.*, vol. 10, 2016.
- [17] A. J. Levine, C. A. Hinckley, K. L. Hilde, S. P. Driscoll, T. H. Poon, J. M. Montgomery, and S. L. Pfaff, "Identification of a cellular node for motor control pathways," *Nat. Neurosci.*, vol. 17, no. 4, pp. 586–593, 2014.
- [18] S. Noetscher, G. Htet, A. T., Markov, "N-Library of basic triangular surface human body meshes from male subjects," *NEVA Electromagn. Ltd. Liabil. Co. LCC.*, 2012.